

Electronic Supplementary Information

Polymorphism of Griseofulvin: Concomitant Crystallization from the melt and Single Crystal Structure of a Metastable Polymorph with Anomalously Large Thermal Expansion

Yuan Su^a, Jia Xu^a, Qin Shi^a, Lian Yu^c, Ting Cai^{a, b,*}

^aState Key Laboratory of Natural Medicines, Department of Pharmaceutics, China Pharmaceutical University, Nanjing, 210009, China

^cJiangsu Key Laboratory of Drug Discovery for Metabolic Diseases, China Pharmaceutical University, Nanjing, 210009, China

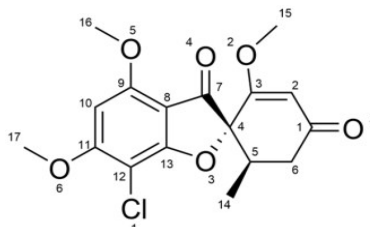
^bSchool of Pharmacy and Department of Chemistry, University of Wisconsin, Madison, 53705, United States

Contents

1. Materials and Methods
2. Characterization of GSF polymorphs
3. Cross-nucleation between GSF forms II and III
4. Determination of thermodynamic relations of GSF polymorphs
5. Structural information of GSF forms I and II
6. Volumetric thermal expansion for some reported organic compounds

1. Materials and Methods

1.1 Materials Used. Griseofulvin(2R,6'S)-7-chloro-2',4,6-trimethoxy-6'-methyl-3H,4'H-spiro [1-benzofuran-2,1'-cyclohex[2]ene]-3,4'-dione) (GSF) was purchased from J&K scientific Co. Ltd., China (purity > 99.0%). Ethanol (AR) was obtained from Jiangsu Hanbon Sci. & Tech. Co., Ltd. All reagents were used as received.



Scheme 1. Molecular Structure of Griseofulvin

1.2 Single-crystal Preparation and X-ray Diffraction Analysis. Single crystals of GSF form II were grown from the supercooled melt of GSF doped with 10 wt % PEO (MW:100,000). ~5 mg of GSF powders were melted on a clean 22 × 22 mm square glass coverslip using a Linkam THMS hot/cold stage. A few small pieces of glass were embedded in the melt to ensure a sample thickness of ~100 μm. A second 15 × 15 mm round coverslip was placed on top of the melted material to create a sandwiched sample. The melted sample was quenched to room temperature by contact with an aluminum block and then reheated to 373 K followed by annealing at this temperature to nucleate for 20 min. The resulting sample was further heated to around 486K to melt all form III and major portion of form II crystals, leading with only a few of form II crystals left in the melt. These remaining form II crystals served as seeds for growing single crystals at 473K. Eventually, one of single crystals of form II which was of adequate size was isolated from the melt by directly peeling off the top coverslip at 473K. At room temperature, the single crystal in sandwiched sample tended to form cracks due to the stress created by the difference of thermal expansion coefficient between coverslip substrate and crystalline GSF. Single crystals of form I were obtained by slow evaporation. 30mg GSF powder dissolved in 5ml hot ethanol. After evaporate at room temperature for two days single crystals of form I were obtained.

Single-crystal X-ray diffraction data were collected on a Bruker D8 Venture diffractometer with Mo K α radiation ($\lambda = 0.71073 \text{ \AA}$). Cell refinement and data reduction were carried out by Bruker SAINT. The crystal structure was solved by direct methods using SHELXS and refined by

full-matrix least-squares using SHELXL in SHELXTL (Sheldrick, 2014). Diffraction quality single crystal for both forms I and II of GSF, were chosen for the experiments. Two complete structural data sets were acquired at 100K, 153K and 298K. In both the forms, the data were corrected for the effects of absorption by a multi-scan method using SADABS. Non-hydrogen atoms were refined anisotropically. The simulated PXRD pattern of form II and the overlap of conformers of GSF polymorphs were calculated by using Mercury 3.9. DIAMOND was used for the creation of figures and analysis of torsional angles.

1.3 Preparation of Amorphous GSF. Amorphous GSF was prepared by melting 2-3 mg of GSF powder at 503K for 3 min on a clean 22×22 mm square microscope coverslip. The liquid was covered with another 15×15 mm round coverslip to yield a film approximately 10 μm thick and was quenched to room temperature by contact with an aluminum block. The amorphous GSF samples prepared in this way was ensured to have no residual crystal nucleus remained by checking the samples at 453K for approximately 20 seconds, monitored by a polarized light microscope equipped with a hot stage. In this study, we avoided any mechanical agitations at the edge of the coverslips during the sample preparation, which enabled the observation of forms II and III in those undisturbed samples.

1.4 Crystallization of GSF Polymorphs in the Melt. Crystal growth rate measurements of GSF form II and III were conducted in the temperature range from 383-483K. The amorphous GSF samples were prepared as described above and partially crystallized at 373K for three to five days in an oven. GSF forms II and III spontaneously nucleated and grown at 373K, and then transferred to a hot stage at the desired temperatures of crystallization

Because cross nucleation of GSF form III on form II was quite dominant and fast in spontaneously nucleated samples at elevated temperatures (above 373K), crystal growth rate measurements of GSF form II were made in “in-situ” seeding crystallization¹. “In-situ” seeded samples were prepared by placing the partially crystallized samples (containing only form II and III) at 483K on a hot stage to completely melt form III and retain form II (m.p. form III = 477K, form II = 486K). Samples were then quenched (cooling at a rate of 50 K /min) to desired temperatures, and the remained form II crystals served as “in situ” seeds for subsequent crystallizations. Crystal growth rates of GSF form III were measured by spontaneously nucleated or cross-nucleated samples. No significant difference was observed between the growth rates

measured from spontaneously nucleated or cross-nucleated crystals. For each measurement, we ensured that the steady-state growth rate was measured (the plot of length change vs. time was linear). The reported growth rate was the average of at least three independent measurements.

1.5 Differential Scanning Calorimetry (DSC). DSC measurements were conducted in a heated aluminum pan using a Q2000 (TA Instruments, New Castle, DE) unit under 50 mL/min N₂ purge. The instrument was calibrated for temperature and enthalpy using indium and sapphire. A total of 2–4 mg of materials was loaded in a heated aluminum pan. The heating rate used in the experiments was 10 K/min and cooling rate was 15K/min. All melting points reported in this study were measured as the values of melting peaks. The thermodynamic relationships between three polymorphs were calculated on the basis of their melting points and enthalpy values.

1.6 Hot-Stage Optical Microscopy (HSM). The crystal morphologies and growth kinetics of GSF in the melt were monitored by using a polarized light microscope (Olympus BX53 microscopy equipped with an Olympus Digital Camera DP26). A Linkam THMS 600 hot stage was equipped on the polarized light microscope to achieve the temperature control.

1.7 Raman Microscopy. Raman microscope was performed with a DXR Raman microscope (Thermo Fisher Scientific, Madison, WI) equipped 780 nm low-power, external stabilized diode laser and CCD detector. With a 50× microscope objective, it offered a laser spot diameter of approximately 1 μm and 3.0-4.1 cm⁻¹ spectral resolution. Spectra were taken at room temperature. The measurement was conducted with a 1 s exposure time for each scan and the final spectrum was the sum of 15 scans with a scanning range from 600 to 1750 cm⁻¹.

1.8 Powder X-ray Diffraction (PXRD). PXRD analysis was conducted at room temperature using D8 Discover A25 X-ray diffractometer (Bruker, Germany). Diffractometer was run at 40 kV and 40 mA with Cu-Kα radiation ($\lambda = 1.54060 \text{ \AA}$). Scans were carried out over a range of 5-35 ° (2θ). The experimental PXRD pattern and the predicted PXRD pattern from the single-crystal structure of form II were compared to confirm the polymorphism of the bulk material.

2. Characterization of GSF polymorphs

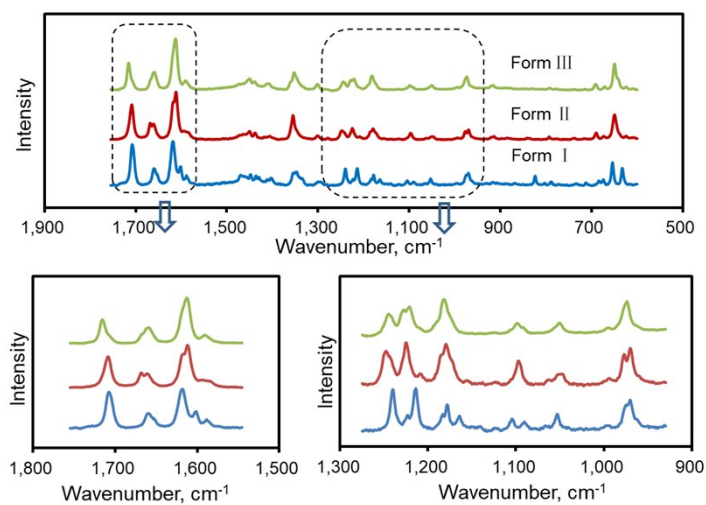


Figure S1. Raman spectroscopy of polymorphic forms of GSF recorded at RT.

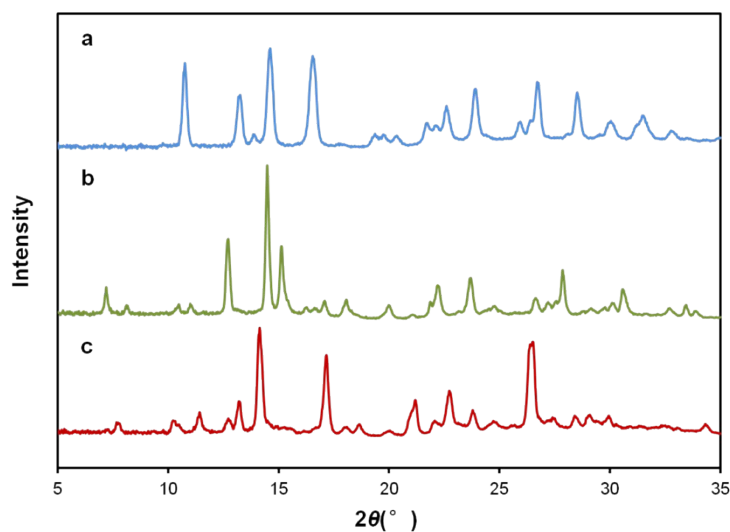


Figure S2. Powder X-ray diffraction patterns of polymorphic forms of GSF recorded at RT. Samples recrystallized from melts were scraped from glass coverslips for the PXRD analysis. (a) GSF form I (original material); (b) GSF form II grew in situ crystallization at 453 K; (c) GSF form III grew in cross-nucleated sample at 453 K.

3. Cross-nucleation between GSF forms II and III

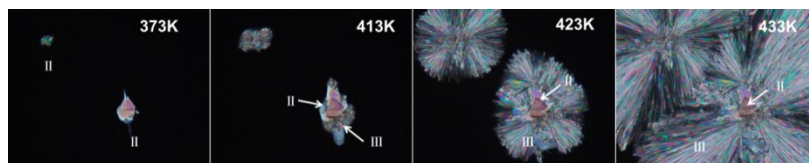


Figure S3. GSF form III nucleated on form II and grew to consume the remaining liquid on heating (10K/min) from 373 to 433 K.

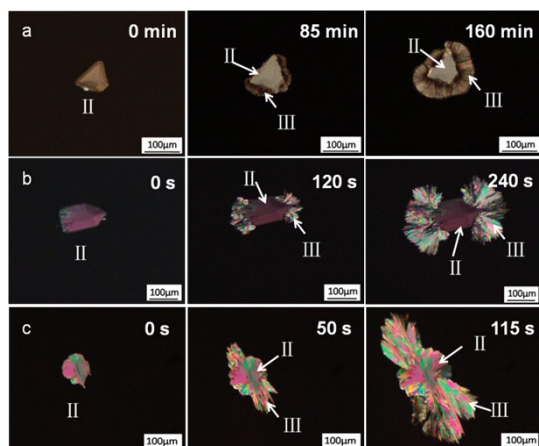


Figure S4. Cross-nucleation between GSF forms II and III in “in-situ” seeding crystallization. Form II crystals were prepared by partially melting samples at 483 K to remove low melting form form III. The un-melted crystals served as “in situ” seeds of form II, and then cooling to desired temperature for growth. (a) 393 K (b) 423 K (c) 433 K. GSF form III nucleated on form II and encircled it subsequently.

4. Determination of thermodynamic relations GSF polymorphs

The melting temperatures and enthalpies of fusion of GSF polymorphs were determined by using DSC. For concomitant crystallization, pure form III cannot be obtained, and its enthalpy of fusion cannot be readily determined by DSC. Thus, the enthalpy of fusion of GSF form III needed to be calculated. Figure A shows the DSC scans (10 K /min) of GSF with different thermal histories. As shown in Run 1, GSF form I melted at 493K with a enthalpy of fusion of 116 J/g, similar to the reported result². The melt was hold at 503K for 10 min and then cooled to 243K at a rate of 15 K /min to form a glass. Run 2 represents the DSC trace of heating the glass at a rate of 10K/min. It shows a glass transition event with the onset value of 361K, a broad exothermic recrystallization zone ranging from 438K to 463K, and two distinct melting peaks located at 477K and 486K. These two melting peaks are obviously below the melting point of the GSF form I (Run 1), corresponding to the reported melting peaks of GSF forms II and III².

Given the observation on the hot stage, the coexistence of these two melt peaks was a consequence of cross-nucleation of GSF form III by form II. Thus, to obtain pure GSF form II, we heated the glass to 483 K to melt form III and then cooled to 453 K at which no cross-nucleation was observed and annealed for 180 min. Reheating of the annealed sample, Run 3, showed only the endothermic peak at 486K corresponding to the melting peak of GSF form II, with no sign of T_g , indicating that the recrystallization of GSF form II was complete. The enthalpy of fusion of form II can thus be readily determined by integration of the melting peak seen in Run 3 ($\Delta H = 82 \pm 1.1$ J/g). Enthalpy of fusion of GSF form III could not be directly determined by using DSC, since it always crystallizes concomitantly with GSF form II during the recrystallization of melt. We heated the glass to 453 K at which the fastest growth rate of GSF form III was obtained and annealed for 180 min to ensure the complete crystallization. Reheating the fully crystallized sample, Run 4, exhibited only two melt peaks without showing the thermal event of glass transition. A scheme of thermal histories for the samples of Run 3 and 4 was provided in Figure B. The corresponding fraction of GSF form III (X_{III}) is then given by:

$$X_{III} = 1 - X_{II}$$

where X_{II} is the fraction of GSF form II in completely crystallized sample. X_{II} is estimated by comparing the corresponding enthalpy of fusion to that of pure GSF form II ($\Delta H_{II}^m = 82 \pm 1.1$ J/g). The enthalpy of fusion of GSF form III is given by:

$$\Delta H_{III}^m = \Delta H_{III} / X_{III}$$

where ΔH_{III}^m was directly determined by DSC. As a result, the calculated enthalpy of fusion of pure GSF form III was 78 ± 1.6 J/g. The reported enthalpy of fusion was the average of three independent measurements.

In this study, the enthalpies of fusion of forms I (116 ± 0.90 J/g) and II (82 ± 1.1 J/g) directly determined by using DSC were in agreement with the reported results (form I = 120 ± 3 J/g, form II = 81 ± 3 J/g)². However, the calculated enthalpy of fusion of GSF form III (78 ± 1.6 J/g) is much smaller than that of reported value (101 ± 10 J/g)². We considered the difference in enthalpy of fusion of form III was a consequence of different calculation methods. In the previous study by Descamps and coworkers², enthalpy of fusion of GSF form III was determined by reheating the partially crystallized sample. The fraction of form III was calculated by $X_{III} = 1 - X_{II} - X_{am}$, where X_{II} and X_{am} are the fraction of GSF form II and the fraction of quenched liquid not yet recrystallized, respectively. X_{II} was estimated by comparing the corresponding enthalpy of fusion to that of pure form II. X_{am} was estimated by comparing the C_p jump amplitude associated with

the remaining amorphous material to that of the pure quenched liquid. It is plausible that the fraction of GSF form III was underestimated made because of overlooking the crystallization of the remaining amorphous material in reheating process, which caused overestimated $\Delta H_{\text{m}}^{\text{III}}$ successively. Note that our enthalpy of fusion of GSF form III was calculated by reheating the fully crystallized sample. The fraction of GSF form III was given by $X_{\text{III}} = 1 - X_{\text{II}}$ (where X_{II} is the fraction of GSF form II crystallized from the melt). X_{II} can be easily estimated by comparing the corresponding enthalpy of fusion (21 J/g) to that of pure form II (82 J/g). As a result, the composition of the sample after 180 min of annealing at 453K is found to be: $X_{\text{II}} = 25.7\%$, and $X_{\text{III}} = 74.3\%$. The enthalpy associated with the melting of the fraction of form III was found to be 57.8 J/g, indicating an enthalpy of fusion for pure form III of 77.8J/g. Moreover, we observed significant phase transformation from GSF form III to form II during extended annealing at 463K or higher, but the inverse transformation has never been observed. We believe the enthalpy of fusion of form III measured in this work is more accurate. GSF form II and III form a monotropic set rather than the enantiotropic relationship as suggested in the previous study².

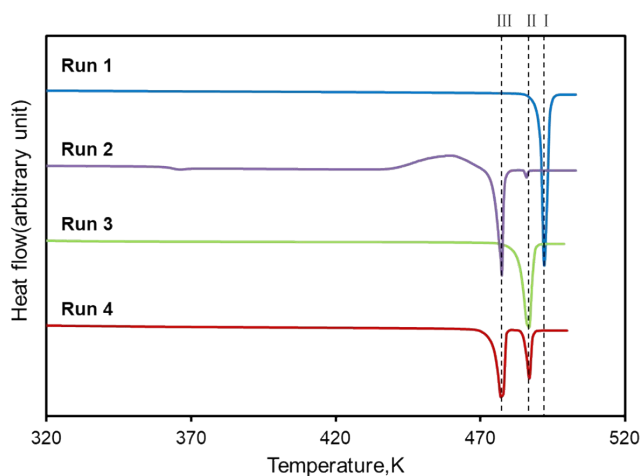


Figure A. DSC scans recorded upon heating samples of GSF at a rate of 10 K/min. Run 1: crystalline form I as supplied, Run 2: melt-quenched glass, Run 3: crystalline form II, Run 4: melt-quenched sample annealed at 453K for 180 min.

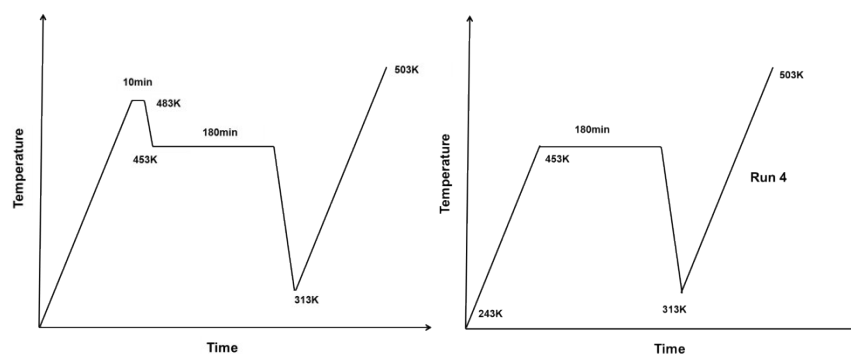


Figure B. A scheme of thermal treatments. (a) Heating the glass to 483K to melt GSF form III, and remaining form II crystals served as seeds. Then cooling to 453K at which no cross-nucleation was observed and annealing for 180 min, GSF form II crystallized completely. A rescanning of the annealed sample was Run 3. (b) Heating the glass to 453 K at which the fastest growth rate of GSF form III was obtained and annealed for 180 min. Rescanning the annealing sample was Run 4.

5. Structural information of GSF forms I and II

Table S1 Crystallographic Data of GSF forms I retrieved from the CSD

CCDC number	1170378	1170379	1170380	259530	866736
Refcode	GRISFL	GRISFL01	GRISFL02	GRISFL03/ GRISFL05	GRISFL04
T, K	283-303	295	295	295(2)	-
Space group	P4 ₁	P4 ₁	P4 ₁	P4 ₁	P4 ₁
Crystal system	tetragonal	tetragonal	tetragonal	tetragonal	tetragonal
a /Å	8.962(1)	8.98	8.967(2)	8.969(2)	8.979(4)
b /Å	8.962(1)	8.98	8.967(2)	8.969(2)	8.979(4)
c /Å	19.895(5)	19.89	19.904(9)	19.951(5)	19.848(7)
α,β,γ/°	90	90	90	90	90
volume/Å ³	1597.92	1603.94	1600.42	1604.9(7)	-
Z	4	4	4	4	4
ρ _{calc} g/cm ³	1.466	-	1.464	1.460	1.46

Table S2 Crystallographic Data of GSF forms I and II

	Form I	Form I	Form I	Form II	Form II	Form II
empirical formula	C ₁₇ H ₁₇ Cl ₁ O	C ₁₇ H ₁₇ Cl ₁ O ₆	C ₁₇ H ₁₇ Cl ₁ O ₆	C ₁₇ H ₁₇ Cl ₁ O ₆	C ₁₇ H ₁₇ Cl ₁ O ₆	C ₁₇ H ₁₇ Cl ₁ O ₆
formula weight	352.75	352.75	352.75	352.75	352.75	352.75
T,K	298	153	100	298	153	100
crystal system	tetragonal	tetragonal	tetragonal	orthorhombic	orthorhombic	orthorhombic
space group	P4 ₁	P4 ₁	P4 ₁	P2 ₁ 2 ₁ 2 ₁	P2 ₁ 2 ₁ 2 ₁	P2 ₁ 2 ₁ 2 ₁
a /Å	8.9799(13)	8.9144(5)	8.9035(6)	11.799(8)	11.6359(6)	11.5984(5)
b /Å	8.9799(13)	8.9144(5)	8.9035(6)	12.007(8)	11.9510(6)	11.9524(6)

$c/\text{\AA}$	19.914(3)	19.6524(12)	19.5908 (13)	24.359(16)	23.6290(12)	23.3284(12)
$\alpha/^\circ$	90	90	90	90	90	90
$\beta/^\circ$	90	90	90	90	90	90
$\gamma/^\circ$	90	90	90	90	90	90
volume/ \AA^3	1605.8(5)	1561.7(2)	1553.0(2)	3450.95(4)	3285.9(3)	3234.0(3)
Z	4	4	4	8	8	8
$\rho_{\text{calc}}/\text{g/cm}^3$	1.459	1.500	1.509	1.358	1.426	1.449

Table S3.Torsional Angles of Molecules in GSF Polymorphs

Conformer	τ_1 (C3-C4-C7-C8)	τ_2 (C7-C4-C5-C14)	τ_3 (O2-C3-C4-O3)
Form I	126.8(2)	58.2(3)	26.5(3)
Form II molecule 1	112.5(4)	44.5(6)	45.5(5)
molecule 2	119.9(4)	46.7(6)	44.2(5)
Atom	numbers	see	Scheme

1.

6. Volumetric thermal expansion for some reported organic compounds

Table S4. Volumetric thermal expansion for some reported organic compounds

Organic compound	α_v , 10 ⁻⁶ K ⁻¹	Temperature zone, K	ratio	ref.
Griseofulvin form I	179	100-298	1.91	this work
Griseofulvin form II	342			
α -p-nitroohenol	156	120-198	1.30	3
β - p-nitroohenol	203			
4,4'-methylenebis(2,6-dimethylaniline) form I	146	148-298	1.61	
4,4'-methylenebis(2,6-dimethylaniline) form II	234			
γ -hexanitrohexaazaisowurtzitane	103	100-298	1.19	
ϵ - hexanitrohexaazaisowurtzitane	123			
(S,S)-3,5-octadiyn-2,7-diol (HT)	271	225-315	1.34	
(S,S)-3,5-octadiyn-2,7-diol (LT)	202			
Tetrolic acid (1D)	265	118-298	1.26	4
Tetrolic acid (0D)	332	118-226		
α -glycine	99	77-298	1.19	
β -glycine	97	77-294	1.17	
γ -glycine	83	77-298	1	
Paracetomal form I Δ	136	20-330	1.28	5
Paracetomal form II Δ	174	100-360		6
Sulfathiazole -I Δ	124	100-300	1.09	7
Sulfathiazole -II Δ	114	100-300	1	
Sulfathiazole -III Δ	120	100-295	1.05	
Sulfathiazole -IV Δ	119	150-295	1.04	
α -chlorpropamide Δ	202	100-295		8
α -2,4- dinitroanisole Δ	178	100-298		9
α -glycylglycin Δ	111	100-295		10
o-terphenyl*	261	-		11
carbamazepine form III \star	190	100-400		12
trichloromesitylene Δ	206	118-262		13
triiodomesitylene Δ	168			
tribromomesitylene Δ	163			
hexamethylbenzene Δ	232			
2,4,6-tris(4-bromophenoxy)-1,3,5-triazine	157	120-298		14

Δ Calculated by PASCAL¹⁵

* α_v is taken to be 3 times of the linear value.

\star Calculate d by the data read from the graph.

Reference

1. J. Tao, K. J. Jones and L. Yu, *Cryst. Growth Des.*, 2007, **7**, 2410-2414.
2. A. Mahieu, J. F. Willart, E. Dudognon, M. D. Eddleston, W. Jones, F. Danede and M. Descamps, *J. Pharm. Sci.*, 2013, **102**, 462-468.
3. S. Bhattacharya and B. K. Saha, *CrystEngComm*, 2014, **16**, 2340.
4. B. K. Saha, *J. Indian Inst. Sci*, 2017, **97**, 177-191.
5. C.C.Wilson, *Zeitschrift für Kristallographie-Crystalline Materials*, 2000, **215**, 693-701.
6. T. N. Drebuschak and E. V. Boldyreva, *Zeitschrift für Kristallographie-Crystalline Materials*, 2004, **219**, 506-512.
7. T. N. Drebuschak, E. V. Boldyreva and M. A. Mikhailenko, *J. Struct. Chem.*, 2008, **49**, 84-94.
8. T. N. Drebuschak, Y. A. Chesalov and E. V. Boldyreva, *Acta Crystallogr. Sect. B*, 2009, **65**, 770-781.
9. H. Takahashi and R. Tamura, *CrystEngComm*, 2015, **17**, 8888-8896.
10. T. N. Drebuschak, E. V. Boldyreva and E. N. Kolesnik, *J. Struct. Chem.*, 2006, **47**, 106-113.
11. C. T. Powell, Y. Chen and L. Yu, *J. Non-Cryst. Solids*, 2015, **429**, 122-128.
12. E. M. Gunn, I. A. Guzei and L. Yu, *Cryst. Growth Des.*, 2011, **11**, 3979-3984.
13. V. G. Saraswatula and B. K. Saha, *Chem. Commun.*, 2015, **51**, 9829-9832.
14. V. G. Saraswatula, M. A. Bhat, S. Bhattacharya and Binoyksaha, *J. Chem. Sci.*, 2014, **126**, 1265-1273.
15. M. J. Cliffe and A. L. Goodwin, *J. Appl. Crystallogr.*, 2012, **45**, 1321-1329.